Super Efimov effect for mass-imbalanced systems

Sergej Moroz and Yusuke Nishida

Phys. Rev. A **90**, 063631 — Published 22 December 2014

DOI: 10.1103/PhysRevA.90.063631

Super Efimov effect for mass imbalanced systems

Sergej Moroz[1,2] and Yusuke Nishida[3]

[1]Department of Physics, University of Washington, Seattle, Washington 98195, USA
[2]Department of Physics, University of Colorado, Boulder, Colorado 80309, USA
[3]Department of Physics, Tokyo Institute of Technology, Ookayama, Meguro, Tokyo 152-8551, Japan

We study two species of particles in two dimensions interacting by isotropic short-range potentials with the interspecies potential fine-tuned to a p-wave resonance. Their universal low-energy physics can be extracted by analyzing a properly constructed low-energy effective field theory with the renormalization group method. Consequently, a three-body system consisting of two particles of one species and one of the other is shown to exhibit the super Efimov effect, the emergence of an infinite tower of three-body bound states with orbital angular momentum $\ell = \pm 1$ whose binding energies obey a doubly exponential scaling, when the two particles are heavier than the other by a mass ratio greater than 4.03404 for identical bosons and 2.41421 for identical fermions. With increasing the mass ratio, the super Efimov spectrum becomes denser which would make its experimental observation easier. We also point out that the Born-Oppenheimer approximation is incapable of reproducing the super Efimov effect, the universal low-energy asymptotic scaling of the spectrum.

PACS numbers: 67.85.Pq, 03.65.Ge, 11.10.Hi

I. INTRODUCTION

When quantum particles interact by a short-range potential with a scattering length much larger than the potential range, they may form universal bound states whose properties are independent of microscopic physics [1–3]. Besides universal N-boson bound states in one dimension [4] and in two dimensions [5], the most remarkable example is the Efimov effect in three dimensions, which predicts the emergence of an infinite tower of three-boson bound states with orbital angular momentum $\ell = 0$ whose binding energies obey the universal exponential scaling [6].

Recently, new few-body universality was discovered at a p-wave resonance in two dimensions [7], which predicts the emergence of an infinite tower of three-fermion bound states with orbital angular momentum $\ell = \pm 1$ whose binding energies obey the universal doubly exponential scaling

$$E_n \propto \exp\bigl(-2e^{3\pi n/4+\theta}\bigr) \tag{1}$$

for sufficiently large $n \in \mathbb{Z}$. It is, to the best of our knowledge, the first physics phenomenon exhibiting the doubly exponential scaling similarly to the hyperinflation in economics [8]. This super Efimov effect summarized in Table I stimulated further theoretical studies in the hyperspherical formalism [9, 10] and its mathematical proof was provided in Ref. [11]. On the other hand, from the experimental perspective, the doubly exponential scaling of the binding energies makes the experimental observation of the super Efimov spectrum challenging.

TABLE I. Comparison of the Efimov effect versus the super Efimov effect [7].

Efimov effect	Super Efimov effect
Three bosons	Three fermions
Three dimensions	Two dimensions
s-wave resonance	p-wave resonance
$\ell = 0$	$\ell = \pm 1$
Exponential scaling	Doubly exponential scaling

In this paper, we extend the super Efimov effect to mass-imbalanced systems, motivated by the fact that the usual Efimov spectrum becomes denser with increasing the mass ratio [12, 13]. This advantage recently made it possible to observe up to three Efimov resonances in ultracold atom experiments with a highly mass-imbalanced mixture of ^{6}Li and ^{133}Cs [14, 15]. Correspondingly, we shall consider two species of particles in two dimensions interacting by isotropic short-range potentials with the interspecies potential fine-tuned to a p-wave resonance.

We first construct an effective field theory in Sec. II that properly captures universal low-energy physics of the system under consideration. This low-energy effective field theory is then employed in Sec. III to analyze a three-body problem consisting of two particles of one species and one of the other with the renormalization group method. Consequently, such a three-body system is shown to exhibit the super Efimov effect when the two particles are heavier than the other by a mass ratio greater than 4.03404 for identical bosons and 2.41421 for identical fermions. We also find that the super Efimov spectrum indeed becomes denser with increasing the mass ratio which would make its experimental observation easier. Finally, we point out in Sec. IV that the Born-Oppenheimer approximation is incapable of reproducing the super Efimov effect, the universal low-energy asymptotic scaling of the spectrum, and Sec. V is devoted to summary and conclusion of this paper. For readers unfamiliar with our renormalization group analysis of the low-energy effective field theory, an explicit model analysis is also presented in Appendix to confirm the predicted super Efimov effect.

II. LOW-ENERGY EFFECTIVE FIELD THEORY

Two species of particles in two dimensions interacting by isotropic short-range potentials are described by

$$H = -\sum_{i=1,2}\int d\boldsymbol{x}\,\psi_i^\dagger(\boldsymbol{x})\frac{\hbar^2\boldsymbol{\nabla}^2}{2m_i}\psi_i(\boldsymbol{x}) + \frac{1}{2}\sum_{i,j=1,2}\int d\boldsymbol{x}d\boldsymbol{y}\,V_{ij}(|\boldsymbol{x}-\boldsymbol{y}|)\psi_i^\dagger(\boldsymbol{x})\psi_j^\dagger(\boldsymbol{y})\psi_j(\boldsymbol{y})\psi_i(\boldsymbol{x}). \tag{2}$$

We assume that the interspecies potential $V_{12}(r)$ is fine-tuned to a p-wave resonance while the intraspecies potentials $V_{11}(r)$ and $V_{22}(r)$ are not. Below we set $\hbar = 1$ and denote total and reduced masses of the two species by $M \equiv m_1 + m_2$ and $\mu \equiv m_1 m_2/(m_1 + m_2)$, respectively.

In order to construct an effective field theory that properly captures universal low-energy physics of the system described by the Hamiltonian (2), low-energy properties of p-wave scattering in two dimensions need to be understood. Potential-independent insights can be obtained from the effective-range expansion for the scattering T-matrix in a p-wave channel [16, 17]:

$$iT_{12} = \frac{2i}{\mu}\frac{2\boldsymbol{p}\cdot\boldsymbol{q}}{-\frac{1}{a_p}-\frac{4\mu\varepsilon}{\pi}\ln\!\left(\frac{\Lambda_p}{\sqrt{-2\mu\varepsilon}}\right)-\sum_{n=2}^{\infty}C_n(-2\mu\varepsilon)^n}. \tag{3}$$

Here $\varepsilon \equiv E - \boldsymbol{k}^2/(2M) + i0^+$ is the collision energy with $\boldsymbol{k}$ being a center-of-mass momentum, $\boldsymbol{p}$ and $\boldsymbol{q}$ are initial and final relative momenta, respectively, while a_p is the scattering area, Λ_p is the effective momentum, and C_n are higher-order shape parameters. In the low-energy limit $\varepsilon \to 0$, the scattering T-matrix (3) right at a p-wave resonance $a_p \to \infty$ reduces to an inspiring form of

$$iT_{12} \to 2\boldsymbol{p}\cdot\boldsymbol{q}\frac{-\pi}{2\mu^2\ln\!\left(\frac{\Lambda_p}{\sqrt{-2\mu\varepsilon}}\right)}\frac{i}{E-\frac{\boldsymbol{k}^2}{2M}+i0^+}. \tag{4}$$

We thus find that the last factor $iD(k) = i/[E - \boldsymbol{k}^2/(2M) + i0^+]$ has exactly the same form as a propagator of free particle whose mass is M, which indicates that the low-energy limit of the resonant p-wave scattering in two dimensions is always described by a propagation of dimer as depicted in Fig. 1 [18]. Correspondingly, the middle factor $(ig)^2 = -\pi/[2\mu^2\ln(\Lambda_p/\sqrt{-2\mu\varepsilon})]$ is interpreted as a p-wave coupling of two scattering particles with the dimer, which has logarithmic energy-dependence and becomes small toward the low-energy limit $\varepsilon \to 0$.

It is then straightforward to write down an effective field theory based on the above low-energy properties of the resonant p-wave scattering in two dimensions, which reads

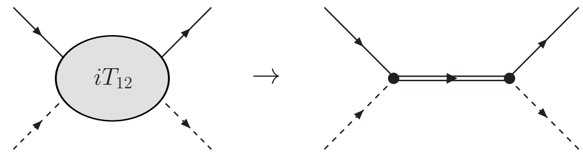

FIG. 1. Low-energy limit of the resonant p-wave scattering in two dimensions reduces to a propagation of dimer (double line) with energy-dependent couplings (dots) [see Eq. (4)]. The solid and dashed lines represent propagators of particles of species 1 and 2, respectively.

$$\begin{aligned}\mathcal{L}_0 &= \sum_{i=1,2}\psi_i^\dagger\left(i\partial_t+\frac{\boldsymbol{\nabla}^2}{2m_i}\right)\psi_i + \sum_{i,j=1,2}\frac{v_{ij}}{2}\psi_i^\dagger\psi_j^\dagger\psi_j\psi_i \\ &+ \sum_{\sigma=\pm}\phi_\sigma^\dagger\left(i\partial_t+\frac{\boldsymbol{\nabla}^2}{2M}-\varepsilon_0\right)\phi_\sigma \\ &+ g\sum_{\sigma=\pm}\phi_\sigma^\dagger\psi_2\left(-i\frac{m_2}{M}\overrightarrow{\nabla}_\sigma + i\frac{m_1}{M}\overleftarrow{\nabla}_\sigma\right)\psi_1 \\ &+ g\sum_{\sigma=\pm}\psi_1^\dagger\left(-i\frac{m_1}{M}\overrightarrow{\nabla}_{-\sigma} + i\frac{m_2}{M}\overleftarrow{\nabla}_{-\sigma}\right)\psi_2^\dagger\phi_\sigma \end{aligned} \tag{5}$$

with $\nabla_\pm \equiv \nabla_x \pm i\nabla_y$. The couplings v_{ij} represent s-wave components of the interspecies and intraspecies interactions, which generally exist without fine-tunings and contribute to low-energy scatterings. We note that the intraspecies s-wave coupling v_{11} (v_{22}) disappears if the particle ψ_1 (ψ_2) obeys the Fermi statistics. The last three terms in the Lagrangian density (5) represent the p-wave component of the interspecies interaction, which is described by a propagation of dimer ϕ_σ with intrinsic angular momentum $\sigma = \pm 1$ as observed above [18]. The interspecies p-wave resonance $a_p \to \infty$ is achieved by fine-tuning the bare detuning parameter ε_0 according to the relationship $1/a_p = \Lambda^2/\pi - 2\varepsilon_0/(\mu g^2)$ with Λ being a momentum cutoff.

The low-energy effective field theory is not yet complete because there are marginal three-body and four-body couplings that can be added to the Lagrangian density (5) [7, 19]. Three-body and four-body scatterings in our low-energy effective description are represented by s-wave couplings between a particle ψ_i and a dimer ϕ_σ and between two dimers, respectively, which are provided by

$$\begin{aligned}\mathcal{L}' &= u_1\sum_{\sigma=\pm}\psi_1^\dagger\phi_\sigma^\dagger\phi_\sigma\psi_1 + u_2\sum_{\sigma=\pm}\psi_2^\dagger\phi_\sigma^\dagger\phi_\sigma\psi_2 \\ &+ w\sum_{\sigma=\pm}\phi_\sigma^\dagger\phi_{-\sigma}^\dagger\phi_{-\sigma}\phi_\sigma + w'\sum_{\sigma=\pm}\phi_\sigma^\dagger\phi_\sigma^\dagger\phi_\sigma\phi_\sigma. \end{aligned} \tag{6}$$

The three-body couplings u_i correspond to the three-body scatterings with total angular momentum $\ell = \pm 1$, while the four-body couplings w and w' correspond to the four-body scatterings with $\ell = 0$ and $\ell = \pm 2$, respectively. We note that w' disappears if the p-wave dimer ϕ_σ obeys the Fermi statistics. The sum of the above

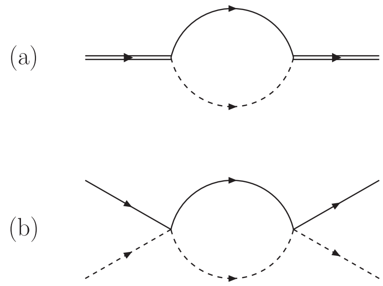

FIG. 2. Feynman diagrams to renormalize the interspecies two-body couplings (a) g and (b) v_{12}. The intraspecies two-body couplings v_{11} and v_{22} are renormalized by Feynman diagrams similar to (b).

two Lagrangian densities $\mathcal{L} = \mathcal{L}_0 + \mathcal{L}'$ now completes the low-energy effective field theory including all marginal couplings (v_{ij}, g, u_i, w, w') consistent with rotation and parity symmetries and the interspecies p-wave resonance, which can be employed to extract universal low-energy physics of the system under consideration (2).

III. RENORMALIZATION GROUP ANALYSIS

A. Two-body sector

The effective-range expansion for the scattering T-matrix indicated that the interspecies p-wave coupling g has logarithmic energy-dependence. This running of the coupling is achieved in the low-energy effective field theory (5) by its renormalization [7, 19]. The Feynman diagram that renormalizes g is depicted in Fig 2(a) and the running of g at a momentum scale $\kappa \equiv e^{-s}\Lambda$ is governed by the renormalization group equation:

$$\frac{dg}{ds} = -\frac{\mu^2}{\pi}g^3 \quad \Rightarrow \quad g^2(s) = \frac{1}{\frac{1}{g^2(0)} + \frac{2\mu^2}{\pi}s}. \tag{7}$$

We thus find that the interspecies p-wave coupling in the low-energy limit $s = \ln \Lambda/\kappa \to \infty$ indeed becomes small logarithmically as $g^2 \to \pi/(2\mu^2 s)$ in agreement with the observation from the effective-range expansion (4).

Similarly, the interspecies and intraspecies s-wave couplings v_{ij} are renormalized by a type of Feynman diagrams depicted in Fig. 2(b). The renormalization group equations that govern the running of v_{ij} and their solutions are provided by

$$\frac{dv_{12}}{ds} = \frac{\mu}{\pi}v_{12}^2 \quad \Rightarrow \quad v_{12}(s) = \frac{1}{\frac{1}{v_{12}(0)} - \frac{\mu}{\pi}s} \tag{8}$$

for the interspecies coupling and

$$\frac{dv_{11}}{ds} = \frac{m_1}{2\pi}v_{11}^2 \quad \Rightarrow \quad v_{11}(s) = \frac{1}{\frac{1}{v_{11}(0)} - \frac{m_1}{2\pi}s} \tag{9}$$

$$\frac{dv_{22}}{ds} = \frac{m_2}{2\pi}v_{22}^2 \quad \Rightarrow \quad v_{22}(s) = \frac{1}{\frac{1}{v_{22}(0)} - \frac{m_2}{2\pi}s} \tag{10}$$

for the intraspecies couplings assuming the Bose statistics obeyed by the particle field ψ_i. Therefore, these s-wave couplings in the low-energy limit $s \to \infty$ also become small logarithmically as $v_{12} \to -\pi/(\mu s)$, $v_{11} \to -2\pi/(m_1 s)$, and $v_{22} \to -2\pi/(m_2 s)$, all of which turn out to be negative indicating effective repulsion regardless of their initial signs for $v_{ij}(0)$, i.e., attractive or repulsive potentials.

B. Three-body sector

We now turn to the renormalization of the three-body couplings u_i in Eq. (6). Without loss of generality, we focus on the renormalization group flow of u_1 because that of u_2 is simply obtained by the exchange of labels $1 \leftrightarrow 2$. In addition to the contribution from the wave function renormalization of ϕ_σ field, there are six distinct diagrams that renormalize u_1 as depicted in Fig. 3. Accordingly, after straightforward calculations [7, 19], the renormalization group equation that governs the running of u_1 is found to be

$$\frac{du_1}{ds} = -\frac{2\mu^2}{\pi}g^2 u_1 + \frac{8\mu^4\nu_1}{\pi m_2^2}g^4 + \frac{2\mu^2}{\pi}g^2 v_{12} + \frac{4\mu^2}{\pi}g^2 v_{11}\delta_{\pm+} \pm \frac{4\mu^2\nu_1}{\pi m_2}g^2 u_1 + \frac{\nu_1}{\pi}u_1^2, \tag{11}$$

where the upper (lower) sign corresponds to the case of bosonic (fermionic) ψ_1 field and $\nu_i \equiv m_i M/(m_i + M)$ is the reduced mass of a particle of species i and a dimer. Each diagram in Fig. 3 contributes to the (a) second, (b) third, (c) fourth, (d,e) fifth, (f) sixth term in the right hand side of Eq. (11), while its first term originates from the wave function renormalization of ϕ_σ field depicted in Fig. 2(a).

By substituting the low-energy asymptotic forms of the two-body couplings g and v_{ij} obtained from Eqs. (7)–(9), the renormalization group equation (11) can be solved analytically and the three-body coupling u_1 in the low-energy limit $s \to \infty$ is provided by

$$su_1(s) \to \mp\frac{\pi}{m_2} - \frac{\pi\gamma}{\nu_1}\cot[\gamma(\ln s - \theta)]. \tag{12}$$

Here θ is a non-universal constant depending on initial conditions for g, v_{ij}, and u_1 at a microscopic scale $s \sim 0$, while $\gamma \equiv \sqrt{\nu_1^2/m_2^2 - \nu_1/\mu - (4\nu_1/m_1)\delta_{\pm+}}$ is the universal exponent expressed in terms of m_1 and m_2 as

$$\gamma = \frac{\sqrt{(m_1+m_2)(m_1^3 - m_1^2 m_2 - 11 m_1 m_2^2 - 5m_2^3)}}{(2m_1+m_2)m_2} \tag{13}$$

in the case of bosonic ψ_1 field (upper sign) and

$$\gamma = \frac{(m_1+m_2)\sqrt{m_1^2 - 2m_1 m_2 - m_2^2}}{(2m_1+m_2)m_2} \tag{14}$$

in the case of fermionic ψ_1 field (lower sign).

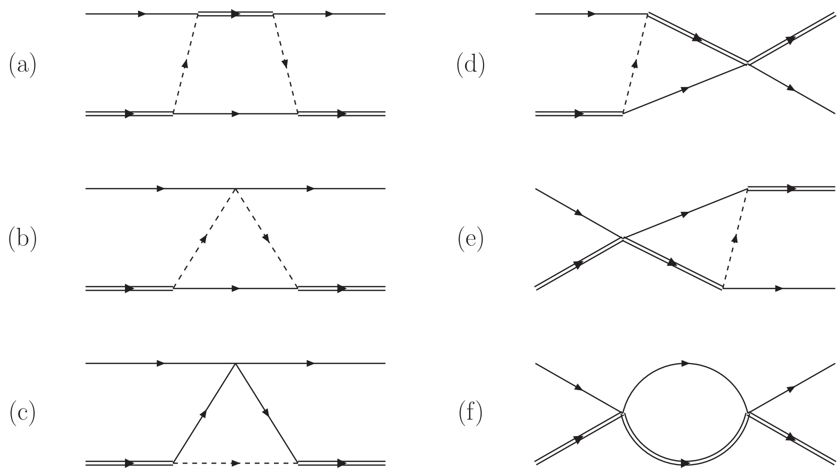

FIG. 3. Feynman diagrams to renormalize the three-body coupling u_1.

When γ is real, the low-energy asymptotic solution (12) for su_1 is a periodic function of $\ln s$ and diverges at $\ln s_n = \pi n/\gamma + \theta$. These divergences in the renormalization group flow of the three-body coupling u_1 indicate the existence of an infinite tower of characteristic energy scales $E_n \propto \kappa_n^2 = e^{-2s_n}\Lambda^2$ in the three-body system consisting of two particles of species 1 and another particle of species 2 with total angular momentum $\ell = \pm 1$. As was confirmed in Ref. [7], these energy scales correspond to binding energies of the three particles which leads to the super Efimov spectrum

$$E_n \propto \exp\bigl(-2e^{\pi n/\gamma+\theta}\bigr) \tag{15}$$

for sufficiently large $n \in \mathbb{Z}$. This super Efimov effect emerges when the majority species 1 is heavier than the minority species 2 and the critical mass ratio is found to be $m_1/m_2 = 4.03404$ from Eq. (13) when the two particles are identical bosons and $m_1/m_2 = 2.41421$ from Eq. (14) when the two particles are identical fermions. In both cases, the universal exponent γ increases monotonously with increasing the mass ratio m_1/m_2, which makes the super Efimov spectrum (15) denser as seen in Fig. 4 for the logarithmic energy ratio $\ln E_{n+1}/\ln E_n \to e^{\pi/\gamma}$ determined by the universal scaling factor.

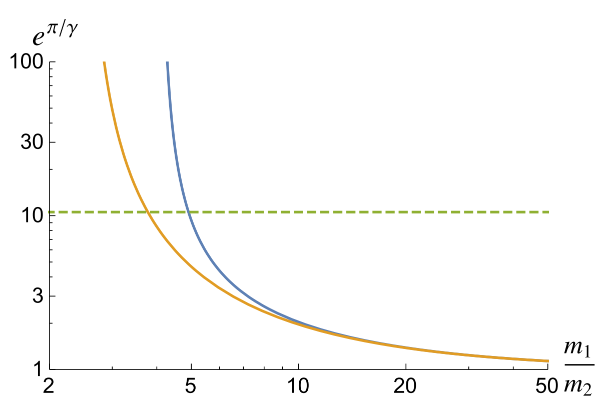

FIG. 4. Universal scaling factor $e^{\pi/\gamma}$ as a function of the mass ratio m_1/m_2 for two identical bosons (upper curve) and fermions (lower curve) with the universal exponent γ determined in Eqs. (13) and (14), respectively. The horizontal dashed line indicates $e^{3\pi/4} \approx 10.55$ corresponding to the universal scaling factor for three identical fermions [7].

So far we considered the most general case where interspecies and intraspecies s-wave interactions v_{ij} exist when they are possible. For the purpose to examine the Born-Oppenheimer approximation in the succeeding section, it is more convenient to consider the simplest case where all s-wave interactions are artificially switched off. By setting $v_{ij} = 0$ in the renormalization group equation (11), the universal exponent γ in the low-energy asymptotic solution (12) for the three-body coupling u_1 is modified into

$$\gamma = \frac{\nu_1}{m_2} = \frac{m_1(m_1+m_2)}{(2m_1+m_2)m_2}. \tag{16}$$

Because γ is always real without s-wave interactions, the super Efimov effect emerges for any mass ratio m_1/m_2. In particular, the super Efimov spectrum (15) becomes independent of whether the two particles are identical bosons or fermions. The super Efimov effect predicted in this simple case will also be confirmed with an explicit model analysis in Appendix.

C. Four-body sector

We then turn to the renormalization of the four-body couplings w and w' in Eq. (6). In addition to the contribution from the wave function renormalization of ϕ_σ field, there are four distinct diagrams that renormalize w and w' as depicted in Fig. 5. Accordingly, after straightforward calculations [7, 19], the renormalization group equations that govern the running of w and w' are found

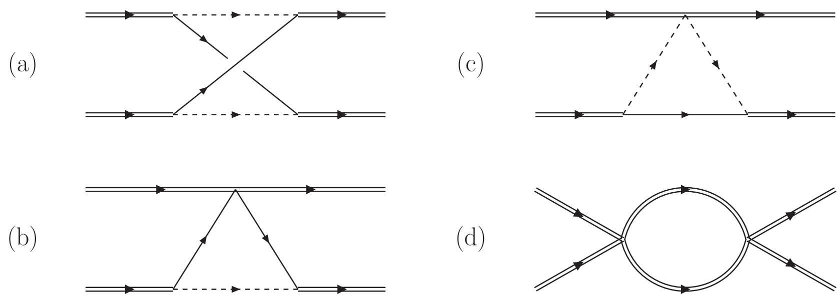

FIG. 5. Feynman diagrams to renormalize the four-body couplings w and w'.

to be

$$\frac{dw}{ds} = -\frac{4\mu^2}{\pi}g^2 w + [(\pm1)_1 + (\pm1)_2]\frac{4\mu^3}{\pi}g^4 + \frac{2\mu^2}{\pi}g^2 u_1 + \frac{2\mu^2}{\pi}g^2 u_2 + \frac{M}{\pi}w^2 \tag{17}$$

and

$$\frac{dw'}{ds} = -\frac{4\mu^2}{\pi}g^2 w' + [(\pm1)_1 + (\pm1)_2]\frac{2\mu^3}{\pi}g^4 + \frac{2\mu^2}{\pi}g^2 u_1 + \frac{2\mu^2}{\pi}g^2 u_2 + \frac{M}{\pi}w'^2. \tag{18}$$

Here the upper (lower) sign in $(\pm1)_i$ corresponds to the case of bosonic (fermionic) ψ_i field and Eq. (18) assumes the Bose statistics obeyed by the p-wave dimer field ϕ_σ. Each diagram in Fig. 5 contributes to the (a) second, (b) third, (c) fourth, (d) fifth terms in the right hand sides of Eqs. (17) and (18), while their first terms originate from the wave function renormalization of ϕ_σ field depicted in Fig. 2(a).

While the renormalization group flows of the four-body couplings w and w' can be studied numerically [7], we defer these analyses to a future work.

IV. BORN-OPPENHEIMER APPROXIMATION

It is well known that the Born-Oppenheimer approximation provides elementary and intuitive understanding of the usual Efimov effect [20]. Therefore, it is worthwhile to examine whether the Born-Oppenheimer approximation is useful as well to understand the super Efimov effect.

In our system under consideration (2), the three-body wave function $\Psi(\boldsymbol{R},\boldsymbol{r})$ describing two particles of species 1 located at $\pm\boldsymbol{R}/2$ and another particle of species 2 located at $\boldsymbol{r}$ in the center-of-mass frame satisfies the Schrödinger equation:

$$\left[-\frac{\boldsymbol{\nabla}_{\boldsymbol{R}}^2}{m_1} - \frac{\boldsymbol{\nabla}_{\boldsymbol{r}}^2}{2m} + V_{11}(R) + V_{12}(r_+) + V_{12}(r_-)\right]\Psi(\boldsymbol{R},\boldsymbol{r}) = E\Psi(\boldsymbol{R},\boldsymbol{r}), \tag{19}$$

where $\boldsymbol{r}_\pm \equiv \boldsymbol{r}\pm\boldsymbol{R}/2$ are interspecies separations and $m \equiv 2m_1m_2/(2m_1+m_2)$ reduces to m_2 at a large mass ratio $m_1/m_2 \gg 1$. The Born-Oppenheimer approximation is based on the factorized wave function

$$\Psi(\boldsymbol{R},\boldsymbol{r}) = \Phi(\boldsymbol{R})\varphi(\boldsymbol{R};\boldsymbol{r}), \tag{20}$$

where the wave function $\varphi(\boldsymbol{R};\boldsymbol{r})$ for the light particle satisfies

$$\left[-\frac{\boldsymbol{\nabla}_{\boldsymbol{r}}^2}{2m_2} + V_{12}(r_+) + V_{12}(r_-)\right]\varphi(\boldsymbol{R};\boldsymbol{r}) = \varepsilon(R)\varphi(\boldsymbol{R};\boldsymbol{r}) \tag{21}$$

with fixed locations of the two heavy particles and the wave function $\Phi(\boldsymbol{R})$ for the two heavy particles in turn satisfies

$$\left[-\frac{\boldsymbol{\nabla}_{\boldsymbol{R}}^2}{m_1} + V_{11}(R) + \varepsilon(R)\right]\Phi(\boldsymbol{R}) = E\Phi(\boldsymbol{R}) \tag{22}$$

with an effective potential $\varepsilon(R)$ generated by the light particle. Corrections to this Schrödinger equation (22) scale as $\sim 1/m_1$ and thus they are usually negligible compared to $\varepsilon(R) \sim 1/m_2$ at a large mass ratio $m_1/m_2 \gg 1$. For simplicity, we also neglect the intraspecies potential $V_{11}(R) \to 0$ and consider only the p-wave component of the interspecies potential $V_{12}(r)$.

The Schrödinger equation (21) with the binding energy $\varepsilon(R) \equiv -\kappa^2/(2m_2)$ potentially admits four bound state solutions for the light particle, whose wave functions outside the potential range $V_{12}(r_\pm) \to 0$ are expressed as

$$\varphi_\pm^x(\boldsymbol{R};\boldsymbol{r}) = K_1(\kappa r_+)\cos[\arg(\boldsymbol{r}_+) - \arg(\boldsymbol{R})] \mp K_1(\kappa r_-)\cos[\arg(\boldsymbol{r}_-) - \arg(\boldsymbol{R})] \tag{23}$$

and

$$\varphi_\pm^y(\boldsymbol{R};\boldsymbol{r}) = K_1(\kappa r_+)\sin[\arg(\boldsymbol{r}_+) - \arg(\boldsymbol{R})] \mp K_1(\kappa r_-)\sin[\arg(\boldsymbol{r}_-) - \arg(\boldsymbol{R})]. \tag{24}$$

We note that $\varphi_+^{x,y}(\boldsymbol{R};\boldsymbol{r})$ $[\varphi_-^{x,y}(\boldsymbol{R};\boldsymbol{r})]$ are even (odd) under the exchange of the two heavy particles $\boldsymbol{R} \to -\boldsymbol{R}$. The interspecies p-wave resonance is achieved by imposing the boundary condition on the light particle wave function $\varphi(\boldsymbol{R};\boldsymbol{r}) \propto 1/r_\pm + O(r_\pm^3)$ at a short distance $r_\pm \sim 1/\Lambda \ll 1/\kappa, R$, which leads to

$$\ln(\Lambda/\kappa) = \pm[K_0(\kappa R) + K_2(\kappa R)] \tag{25}$$

for $\varphi^x_\pm(\boldsymbol{R};\boldsymbol{r})$ and

$$\ln(\Lambda/\kappa) = \pm[K_0(\kappa R) - K_2(\kappa R)] \tag{26}$$

for $\varphi^y_\pm(\boldsymbol{R};\boldsymbol{r})$. Because of $K_2(\kappa R) > K_0(\kappa R) > 0$, these boundary conditions can be satisfied only for $\varphi^x_+(\boldsymbol{R};\boldsymbol{r})$ and $\varphi^y_-(\boldsymbol{R};\boldsymbol{r})$ and their binding energies are found to have the same asymptotic form of

$$\varepsilon_\pm(R) = -\frac{\kappa_\pm^2}{2m_2} \to -\frac{1}{m_2 R^2 \ln(R\Lambda)} \tag{27}$$

for large separation $R\Lambda \to \infty$ between the two heavy particles.

We now solve the Schrödinger equation (22) for the two heavy particles whose wave function can be taken as $\Phi(\boldsymbol{R}) = e^{i\ell \arg(\boldsymbol{R})}\Phi_\ell(R)$ with ℓ corresponding to the total angular momentum of the three particles. We first consider an $\ell = 0$ channel in which bound states are most favored due to the absence of centrifugal barrier. Because the total wave function (20) has to be symmetric (antisymmetric) under the exchange of the two heavy particles $\boldsymbol{R} \to -\boldsymbol{R}$ when they are identical bosons (fermions), only $\varphi^x_+(\boldsymbol{R};\boldsymbol{r})$ $[\varphi^y_-(\boldsymbol{R};\boldsymbol{r})]$ is allowed for the light particle wave function $\varphi(\boldsymbol{R};\boldsymbol{r})$. Then the Schrödinger equation (22) with the effective potential $\varepsilon_+(R)$ $[\varepsilon_-(R)]$ obtained in Eq. (27) leads to an infinite tower of bound states whose binding energies scale as [10, 21]

$$E_n^{(\mathrm{BO})} \propto \exp\!\left(-\frac{m_2\pi^2}{2m_1}n^2\right) \tag{28}$$

for sufficiently large $n \in \mathbb{Z}$ regardless of whether the two heavy particles are identical bosons or fermions. On the other hand, for higher partial-wave channels $\ell \neq 0$, the low-energy asymptotic scaling of the spectrum (28) is terminated around $E \propto e^{-(2/\ell^2)m_1/m_2}$ where the centrifugal barrier overcomes the effective potential (27).

The resulting spectrum from the Born-Oppenheimer approximation differs from the super Efimov spectrum (15) with the universal exponent (16) at a large mass ratio $m_1/m_2 \gg 1$,

$$E_n \propto \exp\!\big(-2e^{(2m_2/m_1)\pi n+\theta}\big), \tag{29}$$

which is the true low-energy asymptotic scaling of the spectrum as was shown in the preceding section. In addition, the Born-Oppenheimer spectrum (28) appears in an $\ell = 0$ channel, while the super Efimov spectrum (29) appears in $\ell = \pm 1$ channels and our analysis predicts no accumulation of infinite bound states toward zero energy in other partial-wave channels. Therefore, we conclude that the Born-Oppenheimer approximation for three-body systems with p-wave resonant interactions in two dimensions is incapable of reproducing the true low-energy asymptotic scaling of the spectrum even at a large mass ratio. This failure of the Born-Oppenheimer approximation may be understood in the following way [22]. When the two heavy particles are separated by a distance R, their characteristic time scale is $\sim m_1 R^2$, while that of the light particle is set by the inverse of its binding energy $\sim m_2 R^2 \ln(R\Lambda)$ from Eq. (27). Therefore, even at a large mass ratio, the light particle cannot adiabatically follow the motion of the two heavy particles for sufficiently large separation $R\Lambda \gtrsim e^{m_1/m_2}$ where the Born-Oppenheimer approximation fails. This argument, however, leaves the possibility that the resulting spectrum (28) may appear as an intermediate scaling for $|E| \gtrsim e^{-2m_1/m_2}\Lambda^2/\mu$.

V. SUMMARY AND CONCLUSION

In this paper, we extended the super Efimov effect to mass-imbalanced systems (2) where two species of particles in two dimensions interact by isotropic short-range potentials with the interspecies potential fine-tuned to a p-wave resonance. Their universal low-energy physics can be extracted by analyzing a properly constructed low-energy effective field theory with the renormalization group method [7, 19]. Consequently, a three-body system consisting of two particles of one species and one of the other is shown to exhibit the super Efimov spectrum,

$$E_n \propto \exp\!\big(-2e^{\pi n/\gamma+\theta}\big) \tag{30}$$

for sufficiently large $n \in \mathbb{Z}$, when the two particles are heavier than the other by a mass ratio greater than 4.03404 for identical bosons [see Eq. (13)] and 2.41421 for identical fermions [see Eq. (14)]. In particular, we found that the universal exponent γ increases monotonously with increasing the mass ratio which makes the super Efimov spectrum denser and thus its experimental observation would become easier with ultracold atoms. For example, a highly mass-imbalanced mixture of ^{6}Li and ^{133}Cs with their interspecies p-wave Feshbach resonances being observed [23] has the universal exponent $\gamma \approx 10.7$ corresponding to the logarithmic energy ratio of $\ln E_{n+1}/\ln E_n \to e^{\pi/\gamma} \approx 1.34$, which is significantly reduced compared to $e^{\pi/\gamma} \approx 10.55$ with $\gamma = 4/3$ for three identical fermions [7].

We also pointed out that the Born-Oppenheimer approximation is incapable of reproducing the super Efimov effect, the universal low-energy asymptotic scaling of the spectrum, even at a large mass ratio for three-body systems with p-wave resonant interactions in two dimensions. The possible reason for this failure of the Born-Oppenheimer approximation was elucidated, while the possibility for the resulting spectrum (28) to appear as an intermediate scaling and then crossover to the asymptotic super Efimov scaling remains to be elucidated in a future work.

ACKNOWLEDGMENTS

We acknowledge many useful discussions with Yvan Castin, Vitaly Efimov, Dmitry S. Petrov, Dam T. Son,

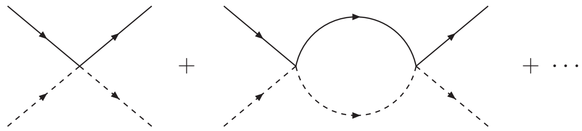

FIG. 6. Feynman diagrams representing the two-body scattering T-matrix (A.2).

and participants in the INT Program on "Universality in few-body systems: Theoretical challenges and new directions." This work was supported by US DOE Grant Number DE-FG02-97ER-41014 and JSPS KAKENHI Grant Number 25887020. Numerical calculations reported in Appendix were performed at the University of Washington Hyak cluster funded by the NSF MRI Grant Number PHY-0922770, the Janus supercomputer funded by the NSF Grand Number CNS-0821794 and the University of Colorado Boulder, and the YITP computer facility in Kyoto University.

Appendix: Model confirmation of the super Efimov effect

The above predictions from our renormalization group analysis of the low-energy effective field theory are all strict as well as universal because we do not need to specify the forms of interspecies and intraspecies potentials in the Hamiltonian (2). However, since some readers may be unfamiliar with our approach, we also present an explicit model analysis to confirm the predicted super Efimov effect by extending that in Ref. [7] to mass-imbalanced systems.

For simplicity, we neglect the intraspecies potentials $V_{11}(r), V_{22}(r) \to 0$ and consider only the p-wave component of the interspecies potential $V_{12}(r)$, which is assumed to be in a separable form of

$$\begin{aligned} H = &\sum_{i=1,2} \int \frac{d\boldsymbol{k}}{(2\pi)^2} \frac{\boldsymbol{k}^2}{2m_i} \psi_i^\dagger(\boldsymbol{k})\psi_i(\boldsymbol{k}) \\ &- v_p \sum_{\sigma=\pm} \int \frac{d\boldsymbol{k}d\boldsymbol{p}d\boldsymbol{q}}{(2\pi)^6} \chi_{-\sigma}(\boldsymbol{q})\chi_\sigma(\boldsymbol{p})\, \psi_1^\dagger\Big(\frac{m_1}{M}\boldsymbol{k}+\boldsymbol{q}\Big) \\ &\times \psi_2^\dagger\Big(\frac{m_2}{M}\boldsymbol{k}-\boldsymbol{q}\Big)\, \psi_2\Big(\frac{m_2}{M}\boldsymbol{k}-\boldsymbol{p}\Big)\, \psi_1\Big(\frac{m_1}{M}\boldsymbol{k}+\boldsymbol{p}\Big) \end{aligned} \tag{A.1}$$

with the p-wave form factor $\chi_\pm(\boldsymbol{p}) \equiv (p_x \pm ip_y)e^{-\boldsymbol{p}^2/(2\Lambda^2)}$ providing a momentum cutoff Λ. By summing an infinite series of Feynman diagrams depicted in Fig. 6, the scattering T-matrix for this model potential is computed as

$$iT_{12} = \frac{2i}{\mu} \frac{2\boldsymbol{p}\cdot\boldsymbol{q}\, e^{-(\boldsymbol{p}^2+\boldsymbol{q}^2)/(2\Lambda^2)}}{\frac{2}{\mu v_p} - \frac{\Lambda^2}{\pi} - \frac{2\mu\varepsilon}{\pi} e^{-2\mu\varepsilon/\Lambda^2} \mathrm{E}_1\big(-\frac{2\mu\varepsilon}{\Lambda^2}\big)}, \tag{A.2}$$

where $\mathrm{E}_1(w) \equiv \int_w^\infty dt\, e^{-t}/t$ is the first-order exponential integral. The interspecies p-wave resonance $a_p \to \infty$ is achieved by fine-tuning the bare p-wave coupling v_p according to the relationship $1/a_p = \Lambda^2/\pi - 2/(\mu v_p)$, which is obtained by comparing the computed scattering T-matrix (A.2) on shell with the effective-range expansion (3).

We are now ready to analyze a three-body problem consisting of two particles of species 1 and another particle of species 2 right at a p-wave resonance $a_p \to \infty$ in two dimensions. Their scattering T-matrix satisfies a Skorniakov–Ter-Martirosian–type integral equation depicted in Fig. 7, which is expressed in the center-of-mass frame as

$$\begin{aligned} T_{\sigma\sigma'}(E;\boldsymbol{p},\boldsymbol{p}') = &\pm 2\mu \frac{e^{-\frac{M^2+m_1^2}{2M^2}\frac{\boldsymbol{p}^2+\boldsymbol{p}'^2}{\Lambda^2}-\frac{2m_1}{M}\frac{\boldsymbol{p}\cdot\boldsymbol{p}'}{\Lambda^2}}}{\boldsymbol{p}^2+\boldsymbol{p}'^2+\frac{2m_1}{M}\boldsymbol{p}\cdot\boldsymbol{p}'-2\mu E-i0^+} \Big(\frac{m_1}{M}\boldsymbol{p}+\boldsymbol{p}'\Big)_{-\sigma} \Big(\boldsymbol{p}+\frac{m_1}{M}\boldsymbol{p}'\Big)_{\sigma'} \\ &\pm \int \frac{d\boldsymbol{q}}{\pi} \frac{e^{-\frac{M^2+m_1^2}{2M^2}\frac{\boldsymbol{p}^2+\boldsymbol{q}^2}{\Lambda^2}-\frac{2m_1}{M}\frac{\boldsymbol{p}\cdot\boldsymbol{q}}{\Lambda^2}}}{\boldsymbol{p}^2+\boldsymbol{q}^2+\frac{2m_1}{M}\boldsymbol{p}\cdot\boldsymbol{q}-2\mu E-i0^+} \frac{\big(\frac{m_1}{M}\boldsymbol{p}+\boldsymbol{q}\big)_{-\sigma}\sum_{\tau=\pm}\big(\boldsymbol{p}+\frac{m_1}{M}\boldsymbol{q}\big)_\tau T_{\tau\sigma'}(E;\boldsymbol{q},\boldsymbol{p}')}{\Big(\frac{M^2-m_1^2}{M^2}\boldsymbol{q}^2-2\mu E-i0^+\Big) e^{\frac{M^2-m_1^2}{M^2}\frac{\boldsymbol{q}^2}{\Lambda^2}-\frac{2\mu E+i0^+}{\Lambda^2}} \mathrm{E}_1\Big(\frac{M^2-m_1^2}{M^2}\frac{\boldsymbol{q}^2}{\Lambda^2}-\frac{2\mu E+i0^+}{\Lambda^2}\Big)}, \end{aligned} \tag{A.3}$$

where the upper (lower) sign corresponds to the case of bosonic (fermionic) ψ_1 field and $\boldsymbol{p}$ ($\boldsymbol{p}'$) is an initial (final) momentum of a particle of species 1 with respect to the other two particles scattering with an orbital angular momentum σ (σ') $= \pm 1$. When the collision energy E approaches a binding energy $E \to -\kappa^2/\mu < 0$, the above scattering T-matrix factorizes as $T_{\sigma\sigma'}(E;\boldsymbol{p},\boldsymbol{p}') \to Z_\sigma(\boldsymbol{p})Z^*_{\sigma'}(\boldsymbol{p}')/(E+\kappa^2/\mu)$ and the resulting residue function $Z_\sigma(\boldsymbol{p})$ satisfies

$$\begin{aligned} Z_\sigma(\boldsymbol{p}) = \pm \int \frac{d\boldsymbol{q}}{\pi} \frac{e^{-\frac{M^2+m_1^2}{2M^2}\frac{\boldsymbol{p}^2+\boldsymbol{q}^2}{\Lambda^2}-\frac{2m_1}{M}\frac{\boldsymbol{p}\cdot\boldsymbol{q}}{\Lambda^2}}}{\boldsymbol{p}^2+\boldsymbol{q}^2+\frac{2m_1}{M}\boldsymbol{p}\cdot\boldsymbol{q}+2\kappa^2} \times \\ \frac{\big(\frac{m_1}{M}\boldsymbol{p}+\boldsymbol{q}\big)_{-\sigma}\sum_{\tau=\pm}\big(\boldsymbol{p}+\frac{m_1}{M}\boldsymbol{q}\big)_\tau Z_\tau(\boldsymbol{q})}{\Big(\frac{M^2-m_1^2}{M^2}\boldsymbol{q}^2+2\kappa^2\Big) e^{\frac{M^2-m_1^2}{M^2}\frac{\boldsymbol{q}^2}{\Lambda^2}+\frac{2\kappa^2}{\Lambda^2}} \mathrm{E}_1\Big(\frac{M^2-m_1^2}{M^2}\frac{\boldsymbol{q}^2}{\Lambda^2}+\frac{2\kappa^2}{\Lambda^2}\Big)}. \end{aligned} \tag{A.4}$$

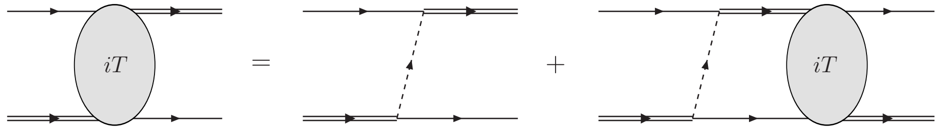

FIG. 7. Feynman diagrams representing the three-body scattering T-matrix (A.3).

It is easy to see that $Z_+(\boldsymbol{p}) = e^{i(\ell-1)\arg(\boldsymbol{p})} z_+(p)$ couples to $Z_-(\boldsymbol{p}) = e^{i(\ell+1)\arg(\boldsymbol{p})} z_-(p)$ with ℓ corresponding to the total angular momentum of the three particles. Below we focus on an $\ell = +1$ channel in which the super Efimov effect was shown to emerge, while solutions in an $\ell = -1$ channel are simply obtained by the exchange of labels $+ \leftrightarrow -$.

The two coupled integral equations (A.4) can be solved analytically in the low-energy limit $\kappa/\Lambda \to 0$ with the leading-logarithm approximation [7, 24, 25]. We assume that the integral is dominated by the region $\kappa \ll q \ll \Lambda$ and split the integral into two parts, $\kappa \ll q \ll p$ and $p \ll q \ll \Lambda$, where a sum of p and q in the integrand is replaced with whichever is larger. Accordingly, Eq. (A.4) is simplified into

$$\pm\frac{z_+(p)}{\gamma} = \int_\kappa^p \frac{dq}{q}\,\frac{z_+(q)}{\ln\Lambda/q} + \int_p^{\epsilon\Lambda} \frac{dq}{q}\,\frac{z_+(q)+z_-(q)}{\ln\Lambda/q}, \tag{A.5a}$$

$$\pm\frac{z_-(p)}{\gamma} = \int_\kappa^p \frac{dq}{q}\,\frac{z_+(q)}{\ln\Lambda/q}, \tag{A.5b}$$

where $\gamma \equiv Mm_1/(M^2 - m_1^2)$ coincides with the universal exponent (16) without s-wave interactions and $\epsilon < 1$ is a positive constant. By changing variables to $P \equiv \ln\ln\Lambda/p$ and $Q \equiv \ln\ln\Lambda/q$ and defining $\lambda \equiv \ln\ln\Lambda/\kappa$, $\eta \equiv \ln\ln 1/\epsilon$, and $\zeta_\pm(P) \equiv z_\pm(p)$, we obtain

$$\pm\frac{\zeta_+(P)}{\gamma} = \int_P^\lambda dQ\,\zeta_+(Q) + \int_\eta^P dQ\,[\zeta_+(Q)+\zeta_-(Q)], \tag{A.6a}$$

$$\pm\frac{\zeta_-(P)}{\gamma} = \int_P^\lambda dQ\,\zeta_+(Q). \tag{A.6b}$$

These two coupled integral equations are solved by [7]

$$\zeta_+(P) = \cos[\mp\gamma(P-\lambda)], \tag{A.7a}$$

$$\zeta_-(P) = \sin[\mp\gamma(P-\lambda)], \tag{A.7b}$$

provided that the boundary condition $\zeta_+(\eta) = \zeta_-(\eta)$ is satisfied. This boundary condition leads to an infinite tower of allowed binding energies $\lambda_n = \pi n/\gamma + \theta$ with $n \in \mathbb{Z}$ for any mass ratio m_1/m_2 regardless of whether the two particles are identical bosons or fermions, which indeed confirms the predicted super Efimov effect (15).

We also solved the two coupled integral equations (A.4) numerically with $\ell = \pm 1$ at mass ratios $m_1/m_2 = 5, 10, 20$ and observed that obtained binding energies asymptotically approach the predicted doubly exponential scaling for each mass ratio. See Table II for the obtained binding energies at $m_1/m_2 = 20$ for two identical bosons corresponding to the upper sign in Eq. (A.4).

TABLE II. Lowest seventeen three-body binding energies $E_n = -\kappa_n^2/\mu$ obtained from Eq. (A.4) for $\ell = \pm 1$, $m_1/m_2 = 20$, and two identical bosons (upper sign). The logarithmic energy ratios asymptotically approach the universal scaling factor $e^{\pi/\gamma} \approx 1.358905074$ with $\gamma = 420/41$ determined in Eq. (16).

n	$\ln(\Lambda/\kappa_n)$	$\ln(\Lambda/\kappa_n)/\ln(\Lambda/\kappa_{n-1})$
0	0.84492	—
1	1.4017	1.6590
2	2.5612	1.8272
3	4.3083	1.6821
4	6.5930	1.5303
5	9.5792	1.4529
6	13.513	1.4107
7	18.740	1.3868
8	25.742	1.3736
9	35.177	1.3665
10	47.939	1.3628
11	65.240	1.3609
12	88.720	1.3599
13	120.61	1.3594
14	163.92	1.3591
15	222.77	1.3590
16	302.73	1.3589
∞	—	1.358905074

[1] E. Nielsen, D. V. Fedorov, A. S. Jensen, and E. Garrido, Phys. Rept. **347**, 373 (2001).
[2] A. S. Jensen, K. Riisager, D. V. Fedorov, and E. Garrido, Rev. Mod. Phys. **76**, 215 (2004).
[3] E. Braaten and H.-W. Hammer, Phys. Rept. **428**, 259 (2006).

[4] J. B. McGuire, J. Math. Phys. **5**, 622 (1964).

[5] H.-W. Hammer and D. T. Son, Phys. Rev. Lett. **93**, 250408 (2004).

[6] V. Efimov, Phys. Lett. B **33**, 563 (1970).

[7] Y. Nishida, S. Moroz, and D. T. Son, Phys. Rev. Lett. **110**, 235301 (2013).

[8] T. Mizuno, M. Takayasu, and H. Takayasu, Physica A **308**, 411 (2002).

[9] A. G. Volosniev, D. V. Fedorov, A. S. Jensen, and N. T. Zinner, J. Phys. B: At. Mol. Opt. Phys. **47**, 185302 (2014).

[10] C. Gao and Z. Yu, arXiv:1401.0965 [cond-mat.quant-gas].

[11] D. K. Gridnev, arXiv:1405.1787 [math-ph].

[12] R. D. Amado and J. V. Noble, Phys. Rev. D **5**, 1992 (1972).

[13] V. Efimov, Sov. Phys. JETP Lett. **16**, 34 (1972); Nucl. Phys. A **210**, 157 (1973).

[14] S.-K. Tung, K. Jimenez-Garcia, J. Johansen, C. V. Parker, and C. Chin, arXiv:1402.5943 [cond-mat.quant-gas].

[15] R. Pires, J. Ulmanis, S. Häfner, M. Repp, A. Arias, E. D. Kuhnle, and M. Weidemüller, Phys. Rev. Lett. **112**, 250404 (2014).

[16] H.-W. Hammer and D. Lee, Phys. Lett. B **681**, 500 (2009); Ann. Phys. **325**, 2212 (2010).

[17] The form of the effective-range expansion up to the second-order in $k \equiv \sqrt{2\mu\varepsilon}$ is not affected as far as the underlying potential $V_{12}(r)$ vanishes faster than r^{-6} at $r \to \infty$. For the van der Waals potential $V_{12}(r) \to -C_6/r^6$, the denominator of Eq. (3) suffers a logarithmic correction of $-[\pi C_6/(32a_p^2)]\, k^2 \ln|k|$, which, however, disappears right at a p-wave resonance $a_p \to \infty$ and thus does not affect the conclusion of this paper.

[18] This specialty of the p-wave resonance in two dimensions is the same as that of the s-wave resonance in four dimensions [26, 27] as was first recognized in Ref. [19].

[19] Y. Nishida, Phys. Rev. D **77**, 061703(R) (2008).

[20] A. C. Fonseca, E. F. Redish, and P. E. Shanley, Nucl. Phys. A **320**, 273 (1979).

[21] The following preprint also appeared when our manuscript was close to completion: M. A. Efremov and W. P. Schleich, arXiv:1407.3352 [quant-ph].

[22] D. S. Petrov, private communication.

[23] M. Repp, R. Pires, J. Ulmanis, R. Heck, E. D. Kuhnle, M. Weidemüller, and E. Tiemann, Phys. Rev. A **87**, 010701(R) (2013).

[24] D. T. Son, Phys. Rev. D **59**, 094019 (1999).

[25] J. Levinsen, N. R. Cooper, and V. Gurarie, Phys. Rev. A **78**, 063616 (2008).

[26] Z. Nussinov and S. Nussinov, Phys. Rev. A **74**, 053622 (2006).

[27] Y. Nishida and D. T. Son, Phys. Rev. Lett. **97**, 050403 (2006); Phys. Rev. A **75**, 063617 (2007).